JOURNAL OF BACTERIOLOGY, Oct. 2010, p. 5329–5340 Vol. 192, No. 20
0021-9193/10/$12.00 doi:10.1128/JB.00729-10

Regulation of Autotrophic CO_2 Fixation in the Archaeon *Thermoproteus neutrophilus*▽†

W. Hugo Ramos-Vera, Valérie Labonté, Michael Weiss, Julia Pauly, and Georg Fuchs*

Mikrobiologie, Fakultät Biologie, Albert-Ludwigs-Universität Freiburg, Freiburg, Germany

Received 22 June 2010/Accepted 1 August 2010

***Thermoproteus neutrophilus*, a hyperthermophilic, chemolithoautotrophic, anaerobic crenarchaeon, uses a novel autotrophic CO_2 fixation pathway, the dicarboxylate/hydroxybutyrate cycle. The regulation of the central carbon metabolism was studied on the level of whole cells, enzyme activity, the proteome, transcription, and gene organization. The organism proved to be a facultative autotroph, which prefers organic acids as carbon sources that can easily feed into the metabolite pools of this cycle. Addition of the preferred carbon sources acetate, pyruvate, succinate, and 4-hydroxybutyrate to cultures resulted in stimulation of the growth rate and a diauxic growth response. The characteristic enzyme activities of the carbon fixation cycle, fumarate hydratase, fumarate reductase, succinyl coenzyme A (CoA) synthetase, and enzymes catalyzing the conversion of succinyl-CoA to crotonyl-CoA, were differentially downregulated in the presence of acetate and, to a lesser extent, in the presence of other organic substrates. This regulation pattern correlated well with the differential expression profile of the proteome as well as with the transcription of the encoding genes. The genes encoding phosphoenolpyruvate (PEP) carboxylase, fumarate reductase, and four enzymes catalyzing the conversion of succinyl-CoA to crotonyl-CoA are clustered. Two putative operons, one comprising succinyl-CoA reductase plus 4-hydroxybutyrate-CoA ligase genes and the other comprising 4-hydroxybutyryl-CoA dehydratase plus fumarate reductase genes, were divergently transcribed into leaderless mRNAs. The promoter regions were characterized and used for isolating DNA binding proteins. Besides an Alba protein, a 18-kDa protein characteristic for autotrophic *Thermoproteales* that bound specifically to the promoter region was identified. This system may be suitable for molecular analysis of the transcriptional regulation of autotrophy-related genes.**

Thermoproteales and *Desulfurococcales* constitute two branches of mostly anaerobic sulfur-metabolizing thermophilic crenarchaea that have been isolated from different volcanic sites (see, e.g., references 24 and 44). They are mostly chemolithoautotrophs and use a new autotrophic CO_2 fixation cycle, as studied in *Ignicoccus hospitalis*, *Pyrolobus fumarii* (*Desulfurococcales*) (14, 27, 30), and *Thermoproteus neutrophilus* (*Thermoproteales*) (6, 46, 49, 50, 51, 57). This autotrophic dicarboxylate/hydroxybutyrate cycle uses pyruvate synthase and phosphoenolpyruvate (PEP) carboxylase to convert acetyl coenzyme A (acetyl-CoA) plus two CO_2 molecules into succinyl-CoA (27, 46) (Fig. 1). The CO_2 acceptor molecule acetyl-CoA is regenerated by converting succinyl-CoA via 4-hydroxybutyrate to two acetyl-CoA molecules. Thus, one additional acetyl-CoA molecule is formed as the starting material for the biosynthesis of cellular building blocks. The regeneration of acetyl-CoA from succinyl-CoA proceeds via the same route as in the autotrophic hydroxypropionate/hydroxybutyrate cycle operating in aerobic *Sulfolobales* (12, 13, 14, 28, 29) and uses the characteristic enzyme 4-hydroxybutyryl-CoA dehydratase (20, 38).

Knowledge of the regulation of autotrophy as well as of the central carbon metabolism in *Archaea*, and especially in *Thermoproteales*, is rather limited (67). In *Thermoproteus tenax*, the genes encoding anabolic PEP synthase, phosphoglycerate kinase, and the classical phosphorylating glyceraldehyde 3-phosphate dehydrogenase, as well as the putative genes encoding fumarate reductase, are upregulated in autotrophically grown cells (19, 61, 68). In contrast, the formation of the catabolic nonphosphorylating glyceraldehyde 3-phosphate dehydrogenase (GAPN) is controlled by the cell energy charge and by intermediates of glycolysis and glucan polymer degradation (18, 36).

Thermoproteus neutrophilus, as whole-cell studies and enzyme activity studies with cell extracts have shown, is a facultative autotroph that actually prefers some organic acids as carbon sources when they become available (46, 49, 50, 51). ^{14}C- and ^{13}C-labeling studies have shown that organic substrates enter the CO_2 fixation cycle and are incorporated into central building blocks according to the positions of the compounds in the cycle (Fig. 1). For instance, the incorporation of acetate dramatically influences the activity of autotrophy-related enzymes, causing a shutdown of the cycle (46).

The marked regulation of *T. neutrophilus* and the availability of its genome sequence (http://jgi.doe.gov/) designate it as a good model for studying the regulation of the central carbon metabolism in *Archaea*. This prompted us to investigate in detail the whole-cell behavior of this organism, the regulation of enzyme activities in response to the added organic carbon source, and the transcriptional regulation of autotrophy-related genes.

* Corresponding author. Mailing address: Mikrobiologie, Fakultät Biologie, Schänzlestr. 1, D-79104 Freiburg, Germany. Phone: 49-761-2032649. Fax: 49-761-2032626. E-mail: georg.fuchs@biologie.uni-freiburg.de.

† Supplemental material for this article may be found at http://jb.asm.org/.

▽ Published ahead of print on 6 August 2010.

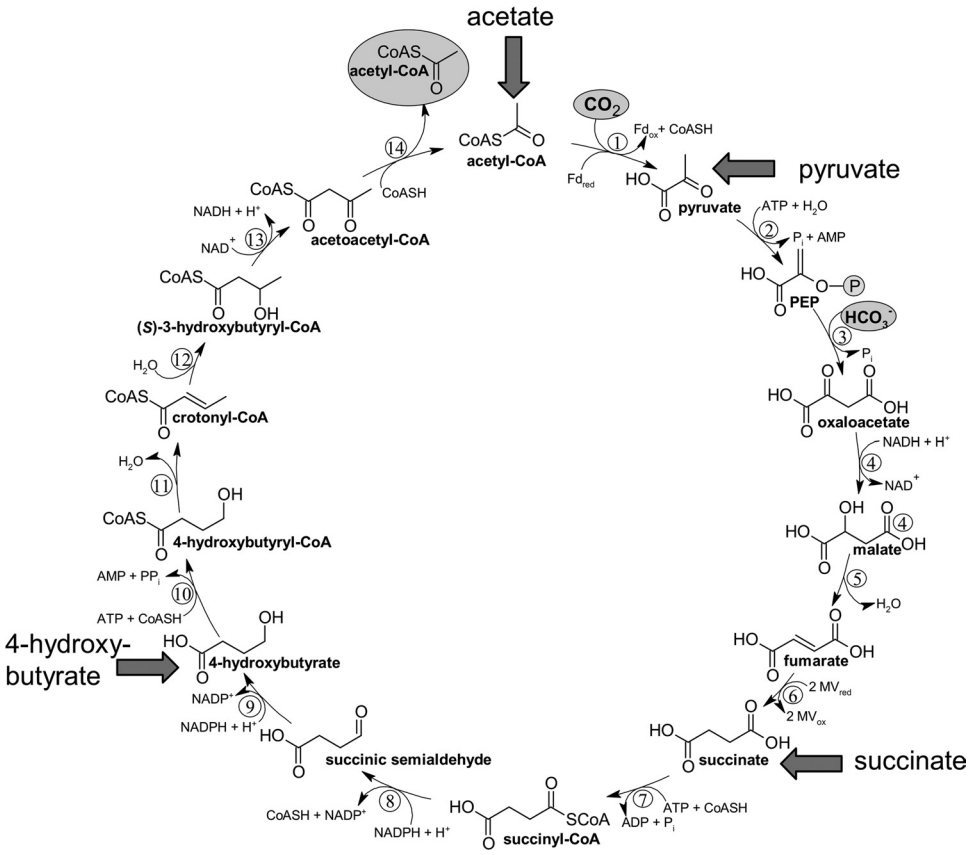

FIG. 1. The autotrophic dicarboxylate/hydroxybutyrate cycle in *T. neutrophilus*. Arrows indicate where organic substrates feed into intermediate pools. Circled numbers represent enzymes as follows (electron carriers are given in parentheses): 1, pyruvate synthase (reduced methyl viologen [MV]); 2, pyruvate:water dikinase; 3, PEP carboxylase; 4, malate dehydrogenase (NADH); 5, fumarate hydratase; 6, fumarate reductase (reduced MV); 7, succinyl-CoA synthetase (ADP forming); 8, succinyl-CoA reductase (NADPH); 9, succinic semialdehyde reductase (NADPH); 10, 4-hydroxybutyrate-CoA ligase (AMP forming); 11, 4-hydroxybutyryl-CoA dehydratase; 12, crotonyl-CoA hydratase; 13, (*S*)-3-hydroxybutyryl-CoA dehydrogenase (NAD^+); 14, acetoacetyl-CoA β-ketothiolase. Fd_{red}, reduced ferredoxin. Reactions 12 and 13 are catalyzed by a bifunctional enzyme. MV may replace ferredoxin as an electron carrier.

MATERIALS AND METHODS

Materials. Chemicals were obtained from Fluka (Neu-Ulm, Germany), Sigma-Aldrich (Deisenhofen, Germany), Qiagen (Hilden, Germany), GE Healthcare (Munich, Germany), VWR (Darmstadt, Germany), and Roth (Karlsruhe, Germany).

Cell material and growth conditions. *Thermoproteus neutrophilus* (DSM 2338) was a kind gift of K. O. Stetter and H. Huber from the culture collection of the Lehrstuhl für Mikrobiologie, Universität Regensburg. It was grown anaerobically and autotrophically on a defined mineral medium with elemental sulfur under gassing with a mixture of 80% H_2 and 20% CO_2 (vol/vol) at 85°C and pH 6.8, as described in reference 49. For comparative studies, cells were grown under the same conditions with the addition of 7 mM acetate, 4-hydroxybutyrate, succinate, pyruvate, DL-malate, fumarate, or glycerol. Cells were harvested in the exponential-growth phase (approximately 1×10^9 cells per ml) by centrifugation and were stored at −70°C until use. Diauxic growth experiments were carried out in a 10-liter glass fermentor. For the determination of total enzyme activity, the cells were grown autotrophically up to a cell density of 3.5×10^8 per ml, and then 5 mM acetate was added.

Preparation of cell extracts. Cell extracts were prepared under anoxic conditions. Cells were suspended in an equal amount of 10 mM Tris-HCl buffer (pH 7.8), and the cell suspension was passed through a chilled French pressure cell at 137 MPa. The lysate was ultracentrifuged for 1 h (100,000 × *g*, 4°C), and aliquots of the supernatant (cell extract) were stored anoxically at −70°C until use. Protein was determined by the Bradford method (16) using bovine serum albumin as the standard.

Enzyme measurements. Spectrophotometric enzyme assays (with a 0.5-ml assay mixture) were performed in 0.5-ml glass cuvettes at 65°C unless otherwise indicated. Anoxic assays were conducted with N_2 as the headspace. Reactions involving NAD(P)H were measured spectrophotometrically at 365 nm ($\varepsilon_{NADH} = 3.4 \times 10^3\ M^{-1}\ cm^{-1}$; $\varepsilon_{NADPH} = 3.5 \times 10^3\ M^{-1}\ cm^{-1}$) (15). Reactions with methyl viologen (MV) were measured at 578 nm ($\varepsilon_{MV} = 9.7 \times 10^3\ M^{-1}\ cm^{-1}$) (69).

Pyruvate:acceptor oxidoreductase (EC 1.2.7.1) was measured anoxically in a mixture containing 100 mM potassium phosphate buffer (pH 7.5), 5 mM $MgCl_2$, 4 mM dithiothreitol (DTT), 4 mM MV, 1 mM CoA, and cell extract. Dithionite was added by syringe until a permanent faint bluish color was obtained. The addition of pyruvate (3 mM) started the reaction.

Fumarate hydratase (EC 4.2.1.2), fumarate reductase (EC 1.3.99.1), succinyl-CoA synthetase (EC 6.2.1.5), succinyl-CoA reductase (EC 1.2.1.-), succinic semialdehyde reductase (E. C. 1.1.1.-), 4-hydroxybutyrate-CoA ligase (EC 6.2.1.-), and 4-hydroxybutyryl-CoA dehydratase (EC 4.2.1.-) were measured as described previously (46).

RT-PCR. Total RNA from 200 mg cells (wet mass) grown autotrophically or grown on acetate and CO_2 was used for reverse transcription-PCR (RT-PCR). RNA was extracted using the TRIzol reagent (Invitrogen, Karlsruhe, Germany) according to the manufacturer's instructions. To remove any genomic DNA present in the samples, 10 μg RNA was treated with 10 U RNase-free DNase I (Fermentas, St. Leon-Rot, Germany) for 30 min at 37°C according to the manufacturer's instructions. RNA was purified by phenol-chloroform-isoamyl alcohol extraction and was resuspended in diethylpyrocarbonate-treated water as described previously (4). RNA concentrations were determined by dilution in water at 260 nm using a Varian Cary 100 Bio UV-vis spectrophotometer. Complete removal of genomic DNA from RNA preparations was verified by amplifying a noncoding region of the genome with cDNA as the template, as follows. Fifty

nanograms of purified total RNA was used to prepare cDNA by using the Sensiscript reverse transcriptase kit (Qiagen) and 10 mM random hexamers for random priming (Applied Biosystems, Darmstadt, Germany). RT-PCR was performed according to the manufacturer's instructions. Gene expression was studied by amplification of gene fragments with cDNA as the template. For analysis of the transcription level, cDNA was diluted in water up to 1,000-fold. PCRs were performed with equal volumes of diluted cDNA (2 μl/50-μl reaction mixture), and the products were analyzed via agarose gel electrophoresis (4). The sequences of the primers used are shown in Table S1 in the supplemental material.

Mapping of the 5′ end of mRNA via primer extension. The transcriptional start sites of the *scr* and *4hbd* genes, encoding succinyl-CoA reductase and 4-hydroxybutyryl-CoA dehydratase, respectively, were analyzed by primer extension. DNA-free total RNA was prepared from autotrophically grown cells as described above for RT-PCR. Primer extension reactions were performed using the primer extension system with avian myeloblastosis virus (AMV) reverse transcriptase (Promega, Mannheim, Germany). The corresponding 5′-Cy5-labeled primer (0.2 pmol) was annealed with total RNA (40 μg) and extended with the reverse transcriptase by following the kit protocol. The lengths of primer extension products were determined by J. Alt-Mörbe (Labor für DNA-Analytik, Freiburg, Germany) using an ALFexpress sequencer. The DNA ladder was produced using primers Cy5-TCTATGGCCCTCCTCACGTCTTCTC and Cy5-CATGAACAG GTTGGTGGTTACG, with *T. neutrophilus* genomic DNA as the template.

Two-dimensional gel electrophoresis and peptide mass fingerprinting. The proteome of *T. neutrophilus* (soluble proteins) was analyzed using conventional 2-dimensional (2-D) gel electrophoresis. Isoelectric focusing (IEF) was performed in an IPGphor isoelectric focusing system (GE Healthcare) using linear gradients of pH 3 to 10, pH 5 to 8, and pH 6 to 11 (Immobiline Dry Strip system [GE Healthcare]; ReadyStrip IPG-Strip [Bio-Rad, Munich, Germany]). Per separation, 0.5 mg protein was applied. Separation in the second dimension was carried out by sodium dodecyl sulfate-polyacrylamide gel electrophoresis (SDS-PAGE) using a 9% or 11% polyacrylamide gel (dimensions, 20 by 20 by 0.1 cm) (34). The protein spots were excised from Coomassie brilliant blue R-stained gels, digested with trypsin, and identified by peptide mass fingerprinting using matrix-assisted laser desorption ionization–time-of-flight mass spectrometry (MALDI-TOF MS) at Toplab (Munich, Germany).

Determination of acetate and succinate levels. Acetate levels were determined spectrophotometrically in a mixture (0.5 ml) containing 100 mM Tris-HCl (pH 7.8), 5 mM $MgCl_2$, 1 mM ATP, 1 mM CoA, 0.4 mM NADH, 1 mM phosphoenolpyruvate (PEP), 2 mM DTT, 1 enzyme unit each of myokinase, lactate dehydrogenase, and pyruvate kinase from rabbit muscle, and 1 enzyme unit of acetyl-CoA synthetase from *Saccharomyces cerevisiae*. The reaction was started with cell-free medium. Succinate levels were determined by high-performance liquid chromatography (HPLC) using an Aminex HPX-87H column (Bio-Rad) with 5 mM H_2SO_4 as the solvent. The Aminex column was equilibrated for 1 h at a flow rate of 0.2 ml min^{-1}, followed by 0.6 ml min^{-1}. Succinate was detected by UV absorbance at 210 nm with a photodiode array detector (Waters, Eschborn, Germany).

DNA affinity purification. DNA binding proteins were purified at room temperature essentially as described previously (22). Cells grown autotrophically or in the presence of acetate were washed with 5 volumes of 50 mM Tris-HCl (pH 7.6) and 50 mM NaCl. After centrifugation, the cells were suspended in 1 volume of 50 mM Tris-HCl (pH 7.6), 1 mM DTT, 10 mM $MgCl_2$, 1 mM EDTA, 10% glycerol (wt/vol), and 10 μM phenylmethylsulfonyl fluoride. The cell suspension was passed through a chilled French pressure cell at 137 MPa. After centrifugation for 1 h (45,000 × *g*, 4°C), the supernatant (cell extract) was stored at −70°C until use.

A 1-ml HiTrap streptavidin HP column (GE Healthcare) was coupled with biotin-labeled DNA, which was generated by PCR using primers 421-422-for-biotin and 421-422-rev (see Table S1 in the supplemental material). Primer 421-422-for-biotin was tagged with biotin by Biomers.net (Ulm, Germany). PCR conditions for the biotin-labeled DNA (promoter DNA) are described below. The PCR product was purified with a QIAquick PCR purification kit. About 130 pmol DNA was coupled to the column. Uncoupled DNA was removed by washing with 10 ml binding buffer containing 20 mM Tris-HCl (pH 7.5), 100 mM NaCl, 1 mM EDTA, 1 mM DTT, 10% glycerin (vol/vol), and 0.05% Triton X-100 (vol/vol). Directly before incubation with the cell extract, the column was equilibrated with 10 volumes of binding buffer at a flow rate of 0.5 ml min^{-1}. Soluble proteins (50 mg) were incubated for 10 min with 100 μg herring sperm DNA (Sigma-Aldrich) and were then applied to the column. After a washing step with 10 ml of binding buffer, bound proteins were eluted with 0.3 and 1 M NaCl in the same buffer. Elution fractions (1 ml) were dialyzed for 24 h in 1 liter of 20 mM Tris-HCl (pH 7.5) at 4°C by using a membrane with a molecular weight cutoff (MWCO) of 3,500 (VWR). The samples were incubated with 12% trichloroacetic acid for 30 min on ice and were then centrifuged for 15 min (16,000 × *g*, 4°C). The pellets were suspended in SDS buffer and were subsequently subjected to SDS-PAGE.

LC–MS-MS and data analysis of the purified DNA binding proteins. For in-gel digestion, the excised gel bands were destained with 30% acetonitrile, shrunk with 100% acetonitrile, and dried in a Eppendorf vacuum concentrator. Digestions with trypsin and elastase were performed overnight at 37°C in 0.05 M NH_4HCO_3 (pH 8). Digestions with thermolysin were performed for 2 h at 60°C in 0.05 M NH_4HCO_3 (pH 8). About 0.1 μg of protease was used for one gel band. Peptides were extracted from the gel slices with 5% formic acid. All liquid chromatography–tandem mass spectrometry (LC–MS-MS) analyses were performed on a quadrupole time-of-flight (Q-TOF) mass spectrometer (Agilent 6520; Agilent Technologies, Böblingen, Germany) coupled to an Agilent 1200 nanoflow system via an HPLC-Chip cube electrospray ionization (ESI) interface. Peptides were separated on an HPLC-Chip system with a 150-mm-long analytical column (inner diameter, 75 μm) and a 40-nl trap column, both packed with Zorbax 300SB C_{18} bonded phase (particle size, 5 μm). Peptides were eluted with a linear acetonitrile gradient of 1%/min at a flow rate of 300 nl/min (starting with 3% acetonitrile). The Q-TOF mass spectrometer was operated in the 2-Ghz extended-dynamic-range mode. MS-MS analyses were performed using data-dependent acquisition mode. After an MS scan (2 spectra/s), a maximum of three peptides were selected for MS-MS (2 spectra/s). Singly charged precursor ions were excluded from selection. Internal calibration was applied using two reference masses. Mascot Distiller, version 2.1, was used for raw data processing and for generating peak lists, essentially with standard settings for the Agilent Q-TOF MS. Mascot Server, version 2.2, was used for database searching with the following parameters: peptide mass tolerance, 15 ppm; MS-MS mass tolerance, 0.02 Da, ^{13}C, 1; enzyme, "trypsin," with 2 uncleaved sites allowed for trypsin, and "none" for elastase and thermolysin; variable modifications, Gln → pyroGlu (N-terminal Glu) and oxidation (methionine). For protein identification, the National Center for Biotechnology Information (NCBI) protein database was used. For protein modification (PTM) analysis, a small custom database containing the protein sequences of the chromatin Alba protein Tneu_1396 was used. All relevant MS-MS spectra were validated manually.

Heterologous expression of Tneu_0751 and Tneu_1396 from *T. neutrophilus* and production of the proteins in *Escherichia coli*. Standard protocols were used for purification, preparation, cloning, transformation, and amplification of DNA (4). Chromosomal DNA was isolated using the illustra Bacteria genomicPrep Mini Spin kit (GE Healthcare). Plasmid DNA was isolated with the QIAprep Spin Miniprep kit (Qiagen). The Tneu_0751 and Tneu_1396 genes were amplified by PCR. Primers are listed in Table S1 in the supplemental material. PCR conditions were as follows: 35 cycles consisting of 30 s of denaturation at 94°C, 30 s of primer annealing at 51°C, and 40 s of elongation at 72°C for Tneu_0751, and 35 cycles consisting of 30 s of denaturation at 94°C, 30 s of primer annealing at 55°C, and 30 s of elongation at 72°C for Tneu_1396. After purification with a QIAquick PCR purification kit, PCR products were treated with restriction enzymes (see Table S1 in the supplemental material) and ligated into the pt7-7 expression vector (58). The constructs were transformed into *Escherichia coli* DH5α. The inserts were sequenced by GATC-Biotech (Konstanz, Germany). The proteins were heterologously expressed in *E. coli* Rosetta 2(DE3) in lysogeny broth medium containing ampicillin and chloramphenicol (100 μg ml^{-1} and 34 μg ml^{-1}, respectively). The culture was induced with 0.1 mM isopropyl-β-D-thiogalactopyranoside at an optical density at 578 nm of 1.8 for Tneu_0751 and 0.5 for Tneu_1396. Cells were grown for an additional 4 h and were harvested by centrifugation for 10 min (12,000 × *g*, 4°C).

Purification of Tneu_0751 and Tneu_1396 from *E. coli*. Cells from the respective overexpression experiment were resuspended in 20 mM Tris-HCl (pH 7.5) containing 50 μg/ml DNase I and were disrupted using a French pressure cell at 137 MPa. The cell lysate was heat precipitated at 92°C for 15 min, incubated for 15 min on ice, and centrifuged (15 min, 16,000 × *g*, 4°C). The supernatant containing Tneu_0751 was dialyzed for 24 h in 1 liter of 10 mM Tris-HCl (pH 7.5) plus 1 mM EDTA using a membrane with an MWCO of 12,000 to 14,000 (Roth). Tneu_0751 was purified using DNA affinity purification as described above. The streptavidin column was coupled with 1.3 nmol biotin-labeled DNA. The 1 M NaCl fractions containing Tneu_0751 were dialyzed for 24 h in 1 liter of 20 mM Tris-HCl (pH 7.5) using an MWCO 3,500 membrane (VWR). Aliquots were stored at −70°C until use. Tneu_1396 was incubated at 37°C for 30 min in 100 mM Tris-HCl (pH 7.5) containing 2.5 mM $MgCl_2$, 0.1 mM $CaCl_2$, DNase I (10 μg/ml), and RNase A (10 μg/ml). After an additional heat precipitation followed by centrifugation, the supernatant was stored at −70°C until use.

EMSA. For electrophoretic mobility shift assays (EMSAs), two DNA probes were generated by PCR. A DNA fragment (127 bp) containing the promoter

regions of the *scr-4hbl* and *4hbd-frd* operons was amplified from *T. neutrophilus* genomic DNA using primers 421-422-for-biotin and 421-422-rev (see Table S1 in the supplemental material). For checking purposes, a DNA fragment (127 bp) was amplified from a region inside the *scr* gene using primers 421-for-biotin and 421-rev. PCR conditions were as follows: 35 cycles consisting of 30 s of denaturation at 94°C, 30 s of primer annealing at 60°C, and 20 s of elongation at 72°C. The PCR products were purified with a QIAquick PCR purification kit. EMSAs were carried out in 20 μl of 10 mM Tris-HCl (pH 7.6) containing 50 mM NaCl, 1 mM DTT, 1 mM EDTA, 10% (wt/vol) glycerol, 100 to 200 ng of DNA, and protein at the indicated concentrations (see Fig. 5). The reaction mixtures were incubated for 30 min at 65°C before separation on an 8% polyacrylamide gel in 40 mM Tris-acetate (pH 8.0)–1 mM EDTA for 3 h at 60 V at room temperature. Subsequently, the gels were poststained for 1 h with 3× GelRed solution (VWR).

The EMSAs were also performed in the presence of either 5 mM adenine nucleotides (AMP, ADP, AMP-PNP, NAD^+, NADH, $NADP^+$, or NADPH); 1 mM CoA, acetyl-CoA, or crotonyl-CoA; or 3 mM acetate, succinate, 4-hydroxybutyrate, pyruvate, phosphoenolpyruvate, DL-malate, or fumarate.

Database search. Query sequences were obtained from the NCBI database. BLAST searches were performed with the NCBI BLAST server (http://www.ncbi.nlm.nih.gov/BLAST/) (1).

RESULTS

Autotrophic growth and growth in the presence of organic substrates. *T. neutrophilus* was cultivated autotrophically as well as in the presence of 7 mM acetate, 4-hydroxybutyrate, succinate, pyruvate, fumarate, DL-malate, or glycerol. Energy sources were hydrogen gas and elemental sulfur; CO_2 was added as a carbon source in each case. Acetate, 4-hydroxybutyrate, succinate, and pyruvate significantly increased the growth rates. The generation time of 8 to 9 h for autotrophic growth was lowered to 5 h for 4-hydroxybutyrate, succinate, and pyruvate, and to 3 h for acetate. This indicates that these organic substrates served as additional carbon sources. DL-Malate, fumarate, and glycerol had no effect on the growth rate, suggesting that they were not assimilated to a great extent.

During growth on acetate, the cultures, when grown to a density of 8.2×10^8 cells per ml, consumed 2.7 mM acetate, which corresponds to 85% of cell carbon. This calculation is based on the cell count of the culture, which was compared to an experimentally determined cell count/cell mass ratio of 1×10^9 cells per ml to 1 mg fresh cell mass per ml. The dry mass content of fresh cells was determined to be 20%; a 50% carbon content of the cells (dry mass) was presupposed. Similarly, succinate cultures consumed 1.4 mM substrate (90% of cell carbon). The remaining cell carbon obviously was obtained from CO_2, the second source of carbon. It has been shown previously that acetate and succinate were not oxidized to volatile CO_2, but served as additional carbon sources (49). This clearly demonstrates the potential of the organism for using external carbon sources, which demands that autotrophic carbon fixation was downregulated by some organic compounds.

Diauxic growth and possible regulation mechanisms. When cells were grown with a limiting amount of acetate (2 to 3.3 mM), diauxic growth was observed (Fig. 2A). The expected typical lag phase, which is observed due to the induced production of enzymes for the second pathway (autotrophy), was quite short. When acetate was used up (<0.1 mM), the growth rate decreased immediately, and enzyme activities required for autotrophic growth appeared in short order (Fig. 2B). Fumarate reductase was chosen as the reporter enzyme for the autotrophic status, since it was strongly regulated (Table 1),

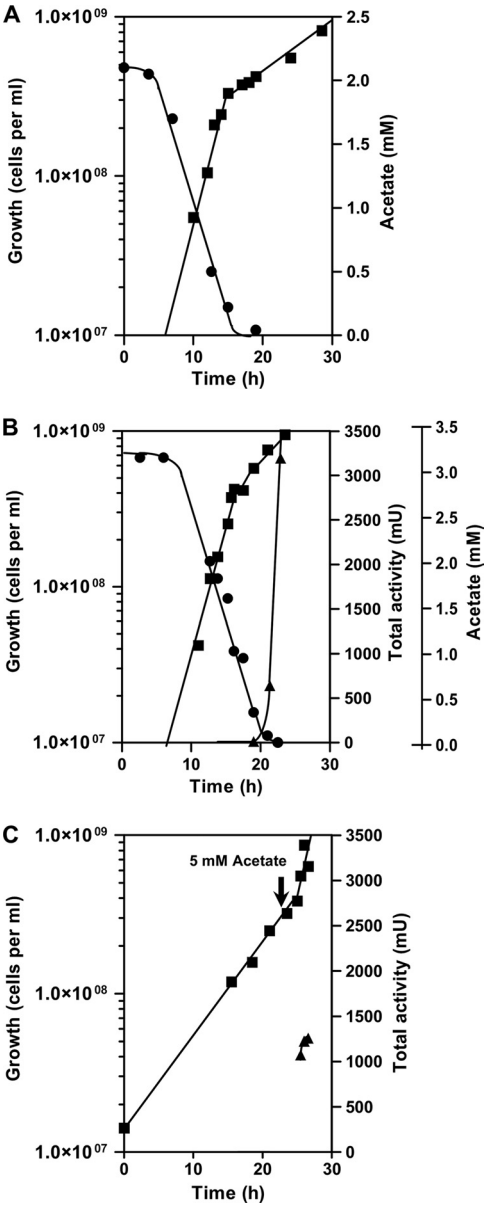

FIG. 2. Relation of the diauxic growth of *T. neutrophilus* and total fumarate reductase activity in 2-liter cultures to the level of acetate in the growth medium. (A) Diauxic growth with CO_2 and H_2 in the presence of limiting amounts of acetate (2 mM). (B) Growth with acetate (3.3 mM) plus CO_2 and H_2. When acetate was consumed, the formation of fumarate reductase set in. (C) Growth with CO_2 and H_2. The arrow marks the time of addition of acetate (5 mM). The total fumarate reductase activity remained nearly constant. Symbols: ■, growth; ●, acetate concentration; ▲, total fumarate reductase activity in the 2-liter culture.

but succinyl-CoA reductase behaved similarly. They were virtually lacking during the acetate growth phase and appeared immediately after acetate depletion. In contrast, pyruvate synthase activity was present before acetate consumption and stayed nearly constant afterwards (not shown). In another experiment, acetate (5 mM) was added to autotrophically growing cells at the mid-exponential-growth phase (Fig. 2C). The addition of acetate almost immediately increased the growth

TABLE 1. Enzymes involved in autotrophic CO_2 assimilation in *T. neutrophilus*[a]

Enzyme[e]	Assay temp (°C)[b]	Sp act (nmol min^{-1} mg of $protein^{-1}$) in cells grown with the following cosubstrate[c]:					Gene(s)[d]
		None	Acetate	4-OH-butyrate	Succinate	Pyruvate	
Pyruvate synthase (oxidized methyl viologen)	65	190	400	330	200	60	Tneu_1795/Tneu_1796/Tneu_1797
Fumarate hydratase	65	500	<10	<10	<10	<10	Tneu_1334/Tneu_1335
Fumarate reductase (reduced methyl viologen)	65	130	<10	<10	<10	<10	Tneu_0423/Tneu_0424
Succinyl-CoA synthetase	65	280	20	20	120	80	Tneu_1463/Tneu_1464
Succinyl-CoA reductase (NADPH)	65	260	20	10	100	60	Tneu_0421
Succinic semialdehyde reductase (NADPH)	65	7,000	900	1,300	3,200	1,000	Tneu_0419
4-Hydroxybutyrate-CoA ligase	85	670	110	140	230	170	Tneu_0420
4-Hydroxybutyryl-CoA dehydratase	85	200	<10	20	90	40	Tneu_0422

[a] Extracts from cells grown with CO_2 as the sole carbon source were compared with extracts from cells grown with CO_2 and another organic carbon source as the cosubstrate. The energy source was H_2 plus S^0 in all cases.
[b] Because of the use of mesophilic coupling enzymes and the instability of some substrates, the indicated assay temperatures were used; the growth temperature was 85°C.
[c] The generation times were 8 h with no substrate, 3 h with acetate, and 5 h with 4-hydroxybutyrate (4-OH-butyrate), succinate, or pyruvate. Values are means from at least duplicate determinations using several separately prepared extracts from different batches of cells. The maximal deviations are approximately 20%.
[d] Subunits of multicomponent enzymes are separated by slashes.
[e] The electron carrier used is given in parentheses.

rate, whereas the total fumarate reductase activity in the culture remained nearly constant. Similar results were obtained with succinyl-CoA reductase and succinic semialdehyde reductase activities (not shown). These observations are congruent with a fast downregulation of the formation of those proteins in the presence of acetate, while the existing proteins are stable and do not become inactivated or proteolytically degraded. Therefore, when the transcription of the corresponding genes was arrested, an increase in cell mass did not contribute to an increase in the total activity of the encoded enzymes. It cannot be decided whether autotrophic upregulation (induction by gene activation) or heterotrophic downregulation (repression by an organic substrate) underlies this regulation, and therefore, both terms are used.

Regulation of enzyme activities. It has been shown previously that the activities of the characteristic enzymes of the dicarboxylate/hydroxybutyrate cycle are downregulated when acetate is present as a substrate (46). A similar regulation was observed with cells grown in the presence of 4-hydroxybutyrate, succinate, or pyruvate (Table 1). Fumarate hydratase and fumarate reductase activities were at least 15-fold downregulated and were hardly detectable. Succinyl-CoA synthetase, succinyl-CoA reductase, succinic semialdehyde reductase, 4-hydroxybutyrate-CoA ligase, and 4-hydroxybutyryl-CoA dehydratase showed approximately 10-fold lower activities in the presence of the organic carbon source. Pyruvate synthase was constitutively formed; it was only slightly downregulated during growth with pyruvate. Acetyl-CoA synthetase was also formed constitutively (46). DL-Malate, fumarate, and glycerol in the growth medium did not affect the enzyme activities (data not shown), a finding in line with the lack of stimulation of the growth rate. The regulation of enzyme activities quite closely meets the requirements of the cells when they are grown with different sources of cell carbon.

Identification of autotrophically upregulated proteins. The sequenced genome of *T. neutrophilus* enabled the use of a proteomic approach to identify proteins specifically involved in CO_2 fixation. Proteins (0.5 mg) in extracts from cells grown on CO_2 alone or on CO_2 plus acetate were separated by 2-dimensional (2-D) gel electrophoresis. Extracts were prepared from different batches of cells. For optimal separation, different polyacrylamide gels as well as different pH gradients were used. After staining with Coomassie brilliant blue R, the gels were scanned, and the protein patterns were visually compared. This allowed the identification of protein spots that were mainly or exclusively autotrophically induced and that were reproducibly found in at least three different batches of cells. All differentially expressed spots from extracts of autotrophically grown cells were analyzed by tryptic peptide fragment mass fingerprinting (PMFP) using matrix-assisted laser desorption ionization–time-of-flight (MALDI-TOF) mass spectrometry. The sequences obtained were mapped to *T. neutrophilus* proteins with high confidence (Mowse scores, >45). Most of the enzymes of the CO_2 fixation cycle were identified as autotrophically induced (Table 2; see also Fig. S1 in the supplemental material). More specifically, 4-hydroxybutyrate-CoA ligase, 4-hydroxybutyryl-CoA dehydratase, and crotonyl-CoA hydratase/3-hydroxybutyryl-CoA dehydrogenase, which participate in the regeneration of acetyl-CoA from succinyl-CoA, were strongly autotrophically induced. PEP synthase and PEP carboxylase were less pronouncedly autotrophically induced but were also detectable in acetate-grown cells. The connection to autotrophy of other induced proteins, such as thermosome proteins and tRNA synthetase, is unclear. Unexpectedly, fumarate reductase and fumarate hydratase could not be identified for all spots, possibly because of overlap with other strongly expressed proteins. Altogether, the proteome pattern is in line with the regulation pattern observed *in vivo* and *in vitro*, and it fully supports the proposed role of the regulated enzymes in the cycle. The proteome data correspond well with the transcriptome analyses presented below.

Organization of the autotrophy-related gene cluster. The organization of a cluster of seven genes that are probably involved in the CO_2 fixation cycle was examined (Fig. 3A). The gene orientation indicated that the gene cluster may be organized in at least two operons and two singly transcribed genes. To identify likely transcriptional units, we performed reverse transcription-PCR (RT-PCR) experiments with cDNA librar-

TABLE 2. Comparative proteome analysis (soluble proteins) of cells grown autotrophically and cells grown in the presence of acetate

Gene	Enzyme[a]	Mass (kDa)	pI	Spot no.	Coverage (%)	Score[b]
Genes encoding enzymes participating in the dicarboxylate/hydroxybutyrate cycle						
Tneu_1795	Pyruvate:ferredoxin oxidoreductase TPP-binding subunit	36.8	8.4	1	52	53
Tneu_1204	Pyruvate-water dikinase (PEP synthase)	89.4	5.8	2	55	301
Tneu_0418	PEP carboxylase	51.4	6.4	3	65	209
Tneu_1509	Malate dehydrogenase (NAD^+)	33.0	7.0	4	70	185
Tneu_1464	Succinyl-CoA synthetase, alpha subunit	30.1	8.9	5	81	184
Tneu_1463	Succinyl-CoA synthetase, beta subunit	41.6	6.0	6	58	164
Tneu_0420	4-Hydroxybutyrate-CoA ligase (AMP forming)	71.2	6.8	7	58	263
Tneu_0422	4-Hydroxybutyryl-CoA dehydratase	55.4	7.8	8	57	198
Tneu_0541	Crotonyl-CoA hydratase/3-hydroxybutyryl-CoA dehydrogenase	72.3	6.3	9	66	350
Genes encoding other proteins						
Tneu_0415	CBS-containing domain protein	15.3	6.2	10	81	131
Tneu_1383	Putative RNA-associated protein	25.9	9.0	11	77	250
Tneu_0708	Putative 3-hexulose-6-phosphate synthase	23.7	6.0	12	77	173

[a] Enzymes involved in the CO_2 assimilation of *T. neutrophilus*, which were induced exclusively under autotrophic growth conditions, as well as some other autotrophic-growth-induced proteins, are listed. For proteome analysis, see Fig. S1 in the supplemental material. TPP, thiamine pyrophosphate.

[b] Calculated as $-10 \times \log(P)$, where P is the probability that the observed match is a random event. Protein scores greater than 45 are considered significant ($P < 0.05$).

ies of DNase-treated RNA derived from autotrophically grown and acetate-grown cells. The primer combinations used for fragments F1 to F5 would amplify DNA fragments containing parts of two adjacent genes that are expected to be cotranscribed (Fig. 3B; see also Table S1 in the supplemental material). All primer pairs yielded a PCR product with genomic DNA, even primer pairs that did not yield a product with RT-PCR (Fig. 3C), showing that all primer pairs fitted well. A noncoding intergene segment (NC) (an arbitrarily chosen 491-bp segment between Tneu_0430 and Tneu_0431) was not amplified with cDNA, excluding the possibility of genomic DNA contamination. As a positive control, a fragment of the isocitrate dehydrogenase gene (PC; 580 bp) was amplified (Fig. 3C).

RT-PCR with cDNA of fragments F1 to F5 indeed gave rise to single products of the expected lengths. In contrast, the primer combination that included regions of *pepc* and *ssr* (fragment F0) did not yield an RT-PCR product, which was expected, because these two genes are oriented in opposite directions. Fragments F2 and F5 each contained part of *4hbd* plus the 74-bp intergenic region and, in addition, 380 bp of *frdA*. The correct amplification to single products showed that no leaky terminator for *4hbd* existed. The results indicated that the genes coding for succinyl-CoA reductase (*scr*) and 4-hydroxybutyrate-CoA ligase (*4hbl*), on one side, and those encoding 4-hydroxybutyryl-CoA dehydratase (*4hbd*) and fumarate reductase subunits A and B (*frdA* and *frdB*), on the other side, were cotranscribed. Note that the gene coding for fumarate hydratase is located elsewhere. These data suggest a sophisticated organization of autotrophy-related genes, which should facilitate coordinate regulation in response to the presence of organic carbon sources.

Regulation of transcription. The postulated regulation of the gene cluster was verified by comparative analysis of cDNA obtained from exponentially grown cells using RT-PCR at different dilutions of the cDNA (Fig. 3D). Cultures were grown either autotrophically or in the presence of acetate. In cells grown in the presence of acetate, the transcript levels for *4hbd-frd* (4-hydroxybutyryl-CoA dehydratase–fumarate reductase genes) and for *scr-4hbl* (succinyl-CoA reductase–4-hydroxybutyrate-CoA ligase genes) were approximately 10-fold downregulated. The unaltered transcript level of the isocitrate dehydrogenase gene served as a control (PC). This coordinated transcription and the differential transcript levels of genes involved in the CO_2 fixation cycle correlate well with the downregulation of the corresponding enzyme activities in acetate-grown cells (Table 1).

Definition of archaeal promoter regions and transcription sites. The 5′ termini of the two divergently transcribed putative operons (the *scr-4hbl* and *4hbd-frdA-frdB* genes) were mapped using primer extension assays (see Fig. S2 in the supplemental material). Cy5-labeled primers were derived from the 5′ region of *scr* or *4hbd* (approximately 100 bases downstream from the translation start codon) and were used in a reverse transcription assay with RNA from autotrophically grown cells. The products of the primer extension were analyzed on a sequencing gel. Both mapped transcripts started at the adenine nucleotide of the translation start codon (ATG), indicating the presence of two leaderless transcripts (*4hbd-frd* and *scr-4hbl*, respectively). Further examination revealed archaeal promoter elements consisting of three parts (Fig. 4). An AT-rich sequence located about 25 bp upstream of the transcriptional start site contained the archaeal TATA box consensus sequence YTTAWA (where Y stands for C or T, and W stands for A or T) (25, 43, 47). The purine-rich transcription factor B (TFB) recognition element (BRE) was adjacent to the TATA box (45). The initiator element (INR) was located around the transcription start site. The minimal requirement for an archaeal initiation site is a pyrimidine-purine dinucleotide at a proper distance from the TATA box, purines being preferred as starting nucleotides (56, 59). Hence, the promoter and tran-

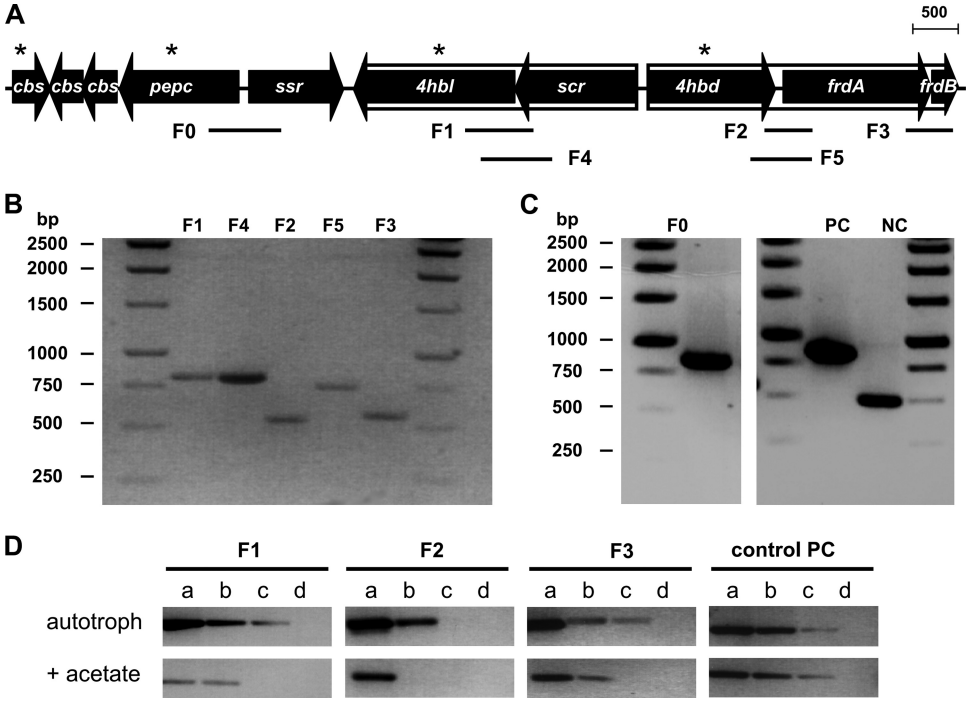

FIG. 3. Transcriptional organization and regulation of a gene cluster in *T. neutrophilus* that is involved in the dicarboxylate/hydroxybutyrate cycle. (A) Structure of the cluster. Lines F1 to F5 represent fragments amplified by PCR using cDNA as a template (see the text). The F0 region gave no amplified fragment. As a negative control, a noncoding region was tested; no fragment was amplified with cDNA. Genes marked by asterisks were upregulated under autotrophic conditions, as evidenced by induced protein spots in 2-D gels. *cbs*, three genes coding for proteins containing cystathionine β-synthase (CBS) domains, *pepc*, PEP carboxylase gene; *ssr*, succinic semialdehyde reductase gene; *4hbl*, 4-hydroxybutyrate-CoA ligase gene; *scr*, succinyl-CoA reductase gene; *4hbd*, 4-hydroxybutyryl-CoA dehydratase gene; *frdA* and *frdB*, genes encoding fumarate reductase subunits A and B. Bar, 500 bp. (B and C) Fragments F1 to F5 were amplified using cDNA as a template (B) or using genomic DNA for the controls (C). Each fragment contained parts of two adjacent genes plus the intergenic region, as follows: F0, *pepc-ssr* (842 bp; intergenic region, 113 bp); F1, *scr-4hbl* (805 bp; intergenic region, 1 bp); F2, *4hbd-frdA* (532 bp; intergenic region, 74 bp); F3, *frdA-frdB* (561 bp; intergenic region, 1 overlapping bp); F4, *scr-4hbl* (804 bp; intergenic region, 1 bp); F5, *4hbd-frdA* (736 bp; intergenic region, 74 bp). PC, positive-control gene for isocitrate dehydrogenase (Tneu_0698); NC, negative control; noncoding region between the Tneu_0430 and Tneu_0431 genes. (D) Induction of genes analyzed via RT-PCR using equal amounts of total RNA isolated from autotrophically (CO_2 and H_2) grown cells or from cells grown in the presence of acetate (acetate plus CO_2 and H_2). For PCRs, cDNA was diluted 1:1 (a), 1:10 (b), 1:100 (c), or 1:1,000 (d) in water.

scription start site characteristics in *T. neutrophilus* conform with the features of other crenarchaea.

Isolation and identification of DNA binding proteins. To identify possible regulator proteins that bind to the promoter regions of the two putative operons (Fig. 4), we enriched proteins binding specifically to the promoter/operator regions by DNA affinity purification. A 127-bp biotinylated promoter/operator DNA fragment (intergenic region between nucleotide +4 of *scr* and nucleotide +2 of *4hbd*) (Fig. 4) was linked to a streptavidin column and incubated with extracts from cells grown autotrophically or in the presence of acetate. Unspecifically bound proteins were eluted with 0.1 M NaCl, whereas specifically bound proteins were eluted with buffers containing 0.3 M NaCl and then 1 M NaCl. The eluted fractions were analyzed by SDS-PAGE (Fig. 5A). There was no significant difference between the two cell extracts tested. Proteins a to e, eluting with 1 M NaCl, were analyzed by nano-LC–MS-MS and were identified by searching in the NCBI protein database. Proteins a and b represent thermosome subunit Tneu_1525 and secretion system protein Tneu_0027, respectively; both contain ATP binding sites. Proteins d and e were identified as small heat shock protein hsp20 (Tneu_1437) and chromatin protein Tneu_1396 (Alba protein), respectively. An RNA polymerase subunit and a 7-kDa chromatin protein (Tneu_1884 and Tneu_1535) were also identified when the whole 1 M NaCl fractions were analyzed.

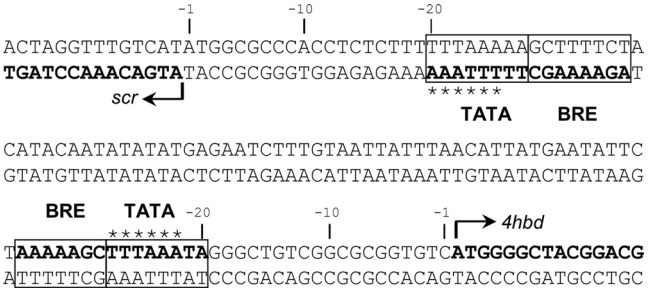

FIG. 4. Promoter definition of the divergently transcribed putative operons *scr-4hbl* and *4hbd-frd*. Arrows indicate the transcription start sites, which correspond to the translation start codons. Putative TATA boxes and archaeal transcription factor B recognition elements (BRE) are boxed. Asterisks indicate the archaeal TATA box consensus sequence YTTAWA.

The Alba protein was highly enriched but eluted mainly at 0.3 M NaCl. Acetylation of the chromatin Alba protein lowers DNA binding affinity (7, 63). Alba protein was digested with

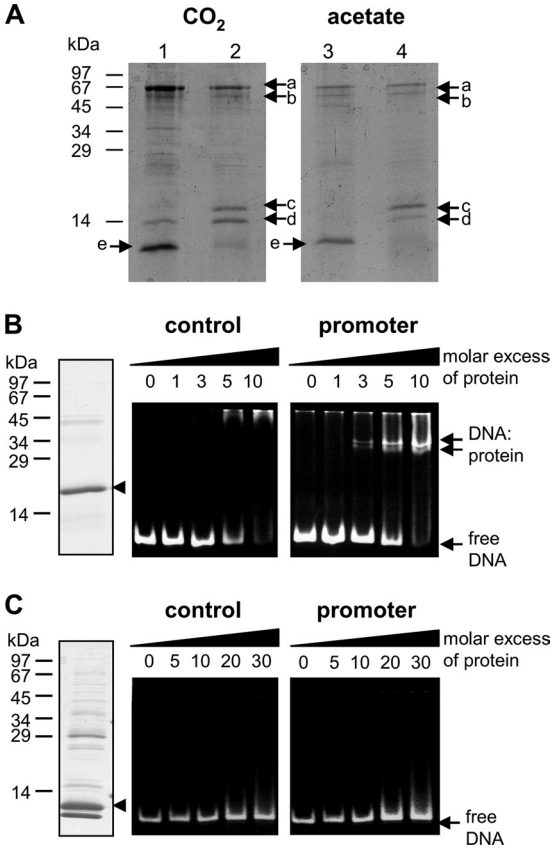

FIG. 5. (A) SDS-PAGE of *T. neutrophilus* proteins eluted from a DNA affinity chromatography column using *scr-4hbl* and *4hbd-frd* promoter/operator probes. Cells were grown on CO_2 or in the presence of acetate. The proteins in lanes 1 and 3 were eluted with 0.3 M NaCl, and those in lanes 2 and 4 were eluted with 1.0 M NaCl. Assignments for proteins a to e are given in the text. (B) Electrophoretic mobility shift assay. (Left) SDS-PAGE of the recombinant Tneu_0751 protein. (Center and right) EMSAs using promoter DNA or control DNA with protein at the indicated molar excesses. (C) SDS-PAGE of recombinant Alba protein and EMSAs as described for panel B. Because of a second start codon inside the gene, a shortened Alba protein was also overexpressed.

trypsin, elastase, and thermolysin, and the posttranslational modifications of this protein were analyzed. It existed as Lys11/12 di- and trimethylated forms, methylated at Lys30/Arg31 and Lys71, and formylated or acetylated at Lys59 and Lys63. Modifications that result in the same nominal mass shift, such as dimethylation and formylation (nominal mass shift, 28 Da) could be distinguished by using high mass accuracy data (65). No significant differences were found between Alba proteins isolated from cells grown autotrophically and those isolated from cells grown in the presence of acetate.

Protein c is an uncharacterized 18-kDa protein (Tneu_0751) that does not contain known conserved domains and is highly conserved only in the autotrophic members of the *Thermoproteales*.

Binding of purified Tneu_0751 and Tneu_1396 to the *scr-4hbl* and *4hbd-frd* promoter/operator regions. To analyze the ability of Tneu_0751 to bind to the *scr-4hbl* and *4hbd-frd* promoter regions, we carried out electrophoretic mobility shift assay (EMSA) analysis. Two DNA fragments were chosen: the 127-bp promoter DNA (intergenic region between nucleotide +4 of *scr* and nucleotide +2 of *4hbd*; also used for DNA affinity purification) and a 127-bp fragment located inside the *scr* gene, used as control DNA. Tneu_0751 was heterologously produced in *E. coli* and was purified. Different amounts of Tneu_0751 were incubated separately with the respective DNA fragments and were separated by nondenaturing polyacrylamide gel electrophoresis. The results of these EMSAs with the promoter and control DNA are shown in Fig. 5B. The migration of the promoter DNA was retarded almost completely by incubation with Tneu_0751 at a molar excess (protein/DNA) of about 10. Two shifted DNA bands were observed. Apparently two protein/DNA complexes were formed, suggesting that there are two Tneu_0751 binding sites in the fragment, corresponding to the two promoter regions. Incubation with control DNA did not result in shifted DNA bands. Hence, Tneu_0751 binds specifically to the *scr-4hbl* and *4hbd-frd* promoters. We tested whether the affinity of Tneu_0751 for the promoter DNA was affected by low-molecular-mass metabolites (adenine nucleotides, CoA, acetyl-CoA, acetate, and further intermediates of the dicarboxylate/hydroxybutyrate cycle, each at 1 to 5 mM) but did not observe any significant effect (not shown).

The chromatin protein Alba (Tneu_1396) was also heterologously produced in *E. coli* and used in EMSAs (Fig. 5C). The migration behaviors of the promoter and control DNAs showed no differences, indicating unspecific protein/DNA interaction.

DISCUSSION

Regulation of the CO_2 fixation cycle. The results of this study show that *T. neutrophilus* behaves as a facultative autotroph that actually prefers organic acids as carbon sources, if they are available. The autotrophic dicarboxylate/hydroxybutyrate cycle is ideally suited for assimilating several common organic acids. The organism lacks the potential for oxidizing organic substrates to CO_2. This lifestyle requires the concerted regulation of autotrophy-related enzymes that are not required, or are only partly required, for the assimilation of the proffered organic substrates. The regulatory effects can be dramatic and at the same time differentiated. For example, growth on acetate rigorously suppressed autotrophy-related enzymes by stopping transcription. Acetyl-CoA synthetase was formed constitutively, allowing immediate trapping of incoming acetate. We showed for fumarate reductase (a strongly regulated target) that this suppression was not due to inactivation or degradation of the enzyme (Fig. 2C). The other enzymes of the cycle that remained present did not interfere with acetate assimilation.

Growth on acetate and pyruvate resulted in a similar regulation pattern. In contrast, succinate shut off fumarate hydratase and fumarate reductase, required for the conversion of malate to succinate, whereas the rest of the autotrophy-related enzymes (notably those required for the conversion of succinyl-CoA to 2 acetyl-CoA molecules and pyruvate synthase) were still active. This suggests that succinate was assimilated via 4-hydroxybutyrate, yielding 2 molecules of acetyl-CoA. 4-Hydroxybutyrate, in addition, downregulated succinyl-CoA syn-

thetase and succinyl-CoA reductase synthesis, which were no longer required for the formation of 4-hydroxybutyrate from succinate.

Comparative proteome analysis identified characteristic autotrophic enzymes as markedly autotrophically induced, except for PEP synthase and PEP carboxylase. An unexpected finding was that the Tneu_0708 protein was autotrophically induced. Its high similarity to 3-hexulose-6-phosphate synthase (HPS) points to a possible participation in the "reverse" ribulose monophosphate pathway for the biosynthesis of ribulose 5-phosphate (Ru5P). This pathway operates in some archaeal strains instead of the oxidative pentose phosphate pathway (32, 42). The relation of this protein and of the induced RNA-associated protein to autotrophy is unclear (Table 2). Interestingly, a protein containing a cystathionine β-synthase (CBS) domain (5, 33) that is encoded by one of the genes of the autotrophy-related gene cluster (Fig. 3) was also induced; this cluster contains two further similar genes. The CBS domain, whose function is unknown to date, may participate in the binding of the adenosyl moiety of coenzymes (adenine and pyridine nucleotides, CoA [or acyl-CoA thioesters]) and may have a role as a structural or regulatory component (53, 64).

Simple modeling of metabolic fluxes under different growth conditions. These observations can be integrated in a simplified model of the carbon flux, which takes into account the metabolites of the autotrophic cycle as well as those of the central carbon metabolism (Fig. 6). Cells grew autotrophically with a generation time of 8 to 9 h, whereas acetate accelerated the growth rate almost 3-fold. A generation time of 9 h requires a minimal *in vivo* specific CO_2 fixation activity of approximately 106 nmol of CO_2 fixed min^{-1} mg of $protein^{-1}$ (46). To generate the universal carbon precursor from 2 CO_2 molecules, a minimal specific activity of 53 nmol min^{-1} mg of $protein^{-1}$ is calculated for the enzymes of the cycle. The measured specific activities of autotrophy-related enzymes match the expected minimal activities.

In Fig. 6A, the autotrophic situation is shown. The metabolic fluxes that lead away from the central precursor metabolites (acetyl-CoA, pyruvate, and oxaloacetate, etc.) to the respective building blocks (presented as open arrows) add up to 100% metabolic flux, which reflects the needs of all cellular building blocks. The magnitudes of the individual fluxes, which divert from the central metabolites (e.g., acetyl-CoA), are given as percentages of the total biosynthetic fluxes; the values given conform to representative bacterial data (41). Since 100% of cellular building blocks are ultimately derived from the CO_2 fixation product acetyl-CoA, running one turn of the cycle adds another 100% metabolic flux. The further away a central metabolite is from acetyl-CoA, the lower the percentage of the flux.

Figure 6B shows the situation of acetate-grown cells; here 100% of precursors are derived from the proffered acetate, which does not need to be regenerated via the cycle. Note, however, that the growth rate is increased almost 3-fold (generation time, 3 h), meaning that the 100% carbon fixation rate is correspondingly higher than that during autotrophic growth. Figure 6C shows the condition of succinate- or 4-hydroxybutyrate-grown cells. The conversion of succinate to two acetyl-CoA molecules requires a 50% relative metabolic flux, because two molecules of this cell carbon precursor are made. The situation for 4-hydroxybutyrate grown cells is identical, except that there is no need to convert succinate to 4-hydroxybutyrate.

When acetate and pyruvate serve as the main carbon sources, the metabolic flux from oxaloacetate via succinyl-CoA and 4-hydroxybutyrate back to acetyl-CoA is obviously dispensable. *Thermoproteus* does not require succinyl-CoA, because porphyrin biosynthesis does not start with succinyl-CoA (Shemin pathway) (54). Instead, the genes coding for the alternative C_5 pathway (21, 31, 52) are present. Succinate is probably assimilated, as indicated in the scheme (Fig. 6C), rather than being oxidized to oxaloacetate. The regulation of succinyl-CoA reductase and 4-hydroxybutyrate-CoA ligase, on the one hand, and that of 4-hydroxybutyryl-CoA dehydratase and fumarate reductase, on the other (Table 1), differ to some extent. This outcome is unexpected, since the two pairs of enzymes are encoded by genes that are cotranscribed.

Surprisingly, malate and fumarate were hardly used as carbon sources, possibly because they were not taken up. This is unexpected, considering the fact that they, like succinate, are C_4-dicarboxylic acids. Alternatively, it is possible that they were taken up and became reductively transformed to succinate to some extent, and that succinate repressed the fumarate hydratase and fumarate reductase activities (which are required for the utilization of these compounds) (Table 1). Glycerol is probably not used because of a lack of glycerol kinase. 4-Hydroxybutyrate certainly is not a common substrate; nevertheless, it exerted pronounced regulatory effects on the production of some dispensable enzymes, such as fumarate hydratase and fumarate reductase.

Molecular aspects of transcriptional regulation in autotrophic *Thermoproteales*. The archaeal initiation of basal transcription involves a promoter consisting of a TATA box about 25 bp upstream of the transcription start site (25, 47, 48) and a BRE. The archaeal RNA polymerase is directed to the promoter by the TATA box-binding protein (TBP) and transcription factor B (9, 10). Different consensus sequences have been established for the TATA box in different branches of the *Archaea* (e.g., TTTTTAAA in *Crenarchaeota* such as *Sulfolobus* species) (59), whereas the BRE is more generally defined as a purine-rich sequence (11). The TATA boxes and BREs proposed in Fig. 4 match these characteristics (8, 35, 45, 56, 60). The transcription start sites of *scr-4hbl* and *4hbd-frd* suggest that the translation of genes that are located first in operons proceeds via leaderless transcripts lacking Shine-Dalgarno (SD) sequences. Initiation on leaderless transcripts is much more common in *Archaea* than in *Bacteria* or *Eukarya* (17, 26, 40, 55, 62) and requires the nondissociated ribosome as well as the initiator tRNA (3, 39). For genes within operons, the SD sequence appears to be particularly important, as evidenced by the prevalence of the SD motifs in those genes. However, we could not identify the SD consensus GGUGA inside the two putative operons of *T. neutrophilus*.

The gene cluster of *T. neutrophilus* containing seven genes encoding six autotrophy-related enzymes and three genes encoding CBS domain-containing proteins is also present in other members of the *Thermoproteales*, such as *Pyrobaculum islandicum* and *Pyrobaculum calidifontis* (see Fig. S3 in the supplemental material). *P. calidifontis* is considered to be a heterotroph (2), but it may be capable of autotrophic growth.

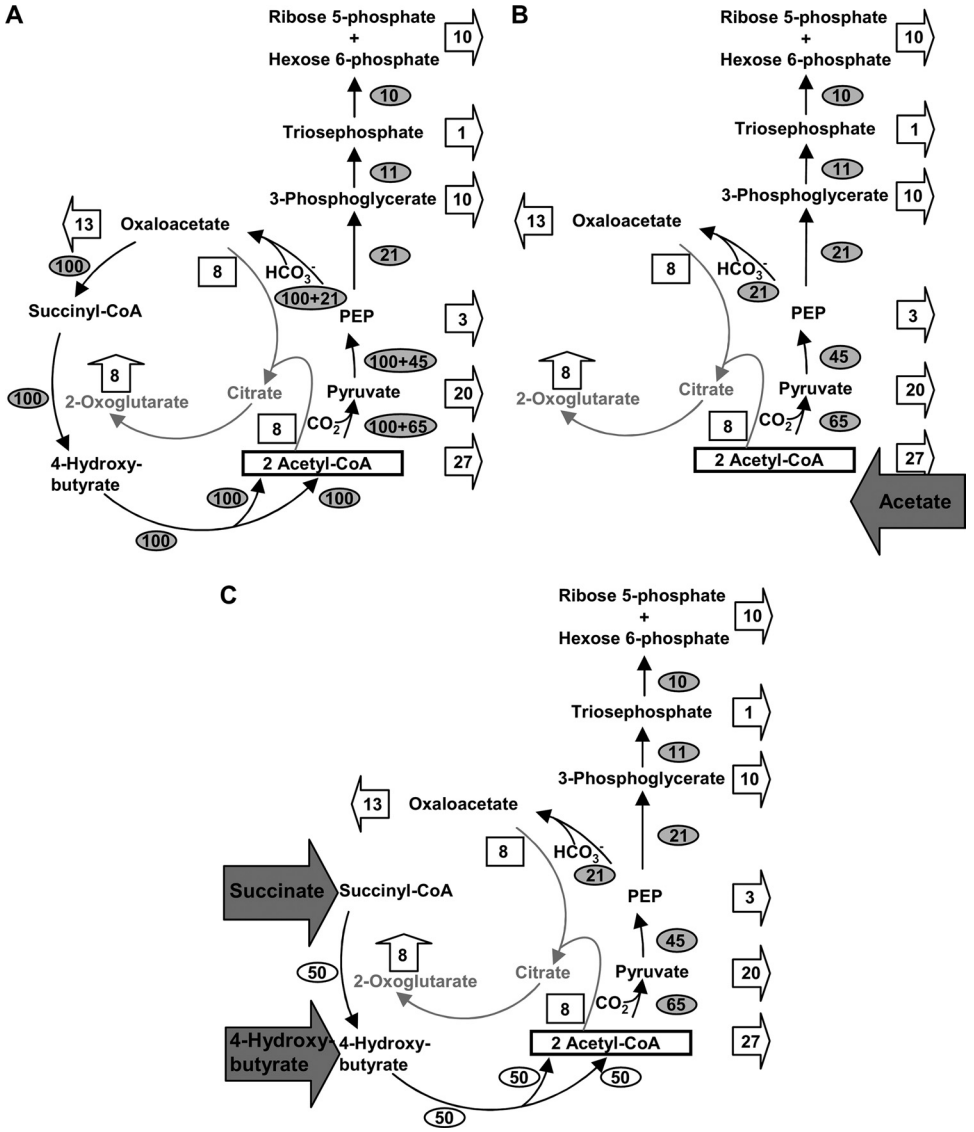

FIG. 6. Metabolic fluxes in autotrophically (CO_2 and H_2) grown cells (A), in cells grown in the presence of acetate (acetate plus CO_2 and H_2) (B), and in cells grown in the presence of succinate or 4-hydroxybutyrate (succinate or 4-hydroxybutyrate plus H_2 and CO_2) (C). Sulfur serves as the electron acceptor in anaerobic respiration. The shaded arrows indicate junctions of organic substrates with the central carbon metabolism. The open arrows symbolize metabolic fluxes away from central carbon metabolites to building blocks. The numbers (given as percentages) refer to 100% metabolic fluxes to the central intermediates from which all building blocks are made. Numbers in open arrows and squares are percentages of total biosynthetic fluxes that start from the central metabolites acetyl-CoA, pyruvate, etc. Numbers in ovals are percentages of metabolic fluxes that are required to supply 100% of the central metabolites. The scheme also shows how pyruvate feeds into this metabolic flux (without giving figures for the metabolic fluxes). The regulation of the enzyme activities under the different growth conditions reflects the biosynthetic demands quite well. For explanations, see the text.

In *Desulfurococcales*, no such gene cluster occurs and no Tneu_0751-like DNA binding protein (see below) exists.

DNA binding and a possible regulator protein. Tneu_0751 has a high affinity for the promoter/operator regions of the putative *scr-4hbl* and *4hbd-frd* operons in *T. neutrophilus*. A highly similar protein (73 to 84% amino acid sequence identity) occurs only in autotrophic members of the *Thermoproteales*, including *P. islandicum*, *Pyrobaculum aerophilum*, *Pyrobaculum arsenaticum*, and *P. calidifontis*. Therefore, this small, 18-kDa protein might act as a transcriptional regulator of key autotrophy-related genes. Because of the constitutive expression of Tneu_0751, some inductor or effector molecule that governs its promoter binding may exist.

Heat shock proteins (Hsp) and the chromatin protein Alba appear to interact with DNA probes in a non-sequence-specific manner. The methylation of specific lysine residues of certain histones alters their DNA binding affinity, which, in turn, affects the expression of some genes. Note that crenarchaea do not possess archaeal histones but have small, basic DNA binding proteins that are thought to fulfill the same functions as histones, based on their physical properties (23). The post-translationally modified chromatin protein Alba may contrib-

ute to transcriptional regulation to a certain extent (7, 37, 63, 66, 70).

How the diverse organic substrates repress the synthesis of autotrophy-related enzymes in such a differential manner remains to be studied. One possible transcription regulator was identified, leaving open the question of how its binding to the promoter region affects transcription and how its function is modified by low-molecular-mass metabolites.

ACKNOWLEDGMENTS

Thanks are due to Nasser Gad'on and Christa Ebenau-Jehle, Freiburg, Germany, for help with growing cells and keeping the lab running and to A. Schlosser, Freiburg, Germany, for MS analysis. We thank K. O. Stetter and H. Huber, Regensburg, Germany, for the kind gift of archaeal strains and Ivan A. Berg for the measurement of 4-hydroxybutyryl-CoA dehydratase. The DOE Joint Genome Institute is acknowledged for the early release of archaeal genomic sequence data.

This work was supported by the Deutsche Forschungsgemeinschaft.

REFERENCES

1. **Altschul, S. F., W. Gish, W. Miller, E. W. Myers, and D. J. Lipman.** 1990. Basic local alignment search tool. J. Mol. Biol. **215:**403–410.
2. **Amo, T., M. L. Paje, A. Inagaki, S. Ezaki, H. Atomi, and T. Imanaka.** 2002. *Pyrobaculum calidifontis* sp. nov., a novel hyperthermophilic archaeon that grows in atmospheric air. Archaea **1:**113–121.
3. **Andreev, D. E., I. M. Terenin, Y. E. Dunaevsky, S. E. Dimtriev, and I. N. Shatsky.** 2006. A leaderless mRNA can bind to mammalian 80S ribosomes and direct polypeptide synthesis in the absence of translation initiation factors. Mol. Cell. Biol. **26:**3164–3169.
4. **Ausubel, F. M., R. Brent, R. E. Kingston, D. D. Moore, J. G. Seidman, J. A. Smith, and K. Struhl.** 1987. Current protocols in molecular biology. John Wiley and Sons, New York, NY.
5. **Bateman, A.** 1997. The structure of a domain common to archaebacteria and the homocystinuria disease protein. Trends Biochem. Sci. **22:**12–13.
6. **Beh, M., G. Strauss, R. Huber, K. O. Stetter, and G. Fuchs.** 1993. Enzymes of the reductive citric acid cycle in the autotrophic eubacterium *Aquifex pyrophilus* and in the archaebacterium *Thermoproteus neutrophilus*. Arch. Microbiol. **160:**306–311.
7. **Bell, S. D., C. H. Botting, B. N. Wardleworth, S. P. Jackson, and M. F. White.** 2002. The interaction of Alba, a conserved archaeal chromatin protein, with Sir2 and its regulation by acetylation. Science **296:**148–151.
8. **Bell, S. D., S. S. Cairns, R. L. Robson, and S. P. Jackson.** 1999. Transcriptional regulation of an archaeal operon in vivo and in vitro. Mol. Cell **4:**971–982.
9. **Bell, S. D., and S. P. Jackson.** 1998. Transcription and translation in *Archaea*: a mosaic of eukaryal and bacterial features. Trends Microbiol. **6:**222–228.
10. **Bell, S. D., and S. P. Jackson.** 2000. Mechanism of autoregulation by an archaeal transcriptional repressor. J. Biol. Chem. **275:**31624–31629.
11. **Bell, S. D., P. L. Kosa, P. B. Sigler, and S. P. Jackson.** 1999. Orientation of the transcription preinitiation complex in archaea. Proc. Natl. Acad. Sci. U. S. A. **96:**13662–13667.
12. **Berg, I. A., D. Kockelkorn, W. Buckel, and G. Fuchs.** 2007. A 3-hydroxypropionate/4-hydroxybutyrate autotrophic carbon dioxide assimilation pathway in *Archaea*. Science **318:**1782–1786.
13. **Berg, I. A., D. Kockelkorn, W. H. Ramos-Vera, R. F. Say, J. Zarzycki, M. Hügler, B. E. Alber, and G. Fuchs.** 2010. Autotrophic carbon fixation in *Archaea*. Nat. Rev. Microbiol. **8:**447–460.
14. **Berg, I. A., W. H. Ramos-Vera, A. Petri, H. Huber, and G. Fuchs.** 2010. Study of the distribution of autotrophic CO_2 fixation cycles in *Crenarchaeota*. Microbiology **156:**256–269.
15. **Bergmeyer, H. U.** 1975. Neue Werte für die molaren Extinktions-Koeffizienten von NADH und NADPH zum Gebrauch im Routine-Laboratorium. Z. Klin. Chem. Klin. Biochem. **13:**507–508.
16. **Bradford, M.** 1976. A rapid and sensitive method for the quantification of microgram quantities of protein utilizing the principle of protein-dye binding. Anal. Biochem. **72:**248–254.
17. **Brenneis, M., O. Hering, C. Lange, and J. Soppa.** 2007. Experimental characterization of *cis*-acting elements important for translation and transcription in halophilic archaea. PloS Genet. **3:**e229.
18. **Brunner, N. A., H. Brinkmann, B. Siebers, and R. Hensel.** 1998. NAD^+-dependent glyceraldehyde-3-phosphate dehydrogenase from *Thermoproteus tenax*. The first identified archaeal member of the aldehyde dehydrogenase superfamily is a glycolytic enzyme with unusual regulatory properties. J. Biol. Chem. **273:**6149–6156.
19. **Brunner, N. A., B. Siebers, and R. Hensel.** 2001. Role of two different glyceraldehyde-3-phosphate dehydrogenases in controlling the reversible Embden-Meyerhof-Parnas pathway in *Thermoproteus tenax*: regulation on protein and transcript level. Extremophiles **5:**101–109.
20. **Buckel, W., and G. T. Golding.** 2006. Radical enzymes in anaerobes. Annu. Rev. Microbiol. **60:**27–49.
21. **Chen, M. W., D. Jahn, G. P. O'Neill, and D. Söll.** 1990. Purification of the glutamyl-tRNA reductase from *Chlamydomonas reinhardtii* involved in δ-aminolevulinic acid formation during chlorophyll biosynthesis. J. Biol. Chem. **265:**4058–4063.
22. **Cramer, A., R. Gerstmeir, S. Schaffer, M. Bott, and B. Eikmanns.** 2006. Identification of RamA, a novel LuxR-type transcriptional regulator of genes involved in acetate metabolism of *Corynebacterium glutamicum*. J. Bacteriol. **188:**2554–2567.
23. **Eichler, J., and M. W. W. Adams.** 2005. Posttranslational protein modification in *Archaea*. Microbiol. Mol. Biol. Rev. **69:**393–425.
24. **Fischer, F., W. Zillig, K. O. Stetter, and G. Schreiber.** 1983. Chemolithoautotrophic metabolism of anaerobic extremely thermophilic archaebacteria. Nature **301:**511–513.
25. **Hain, J., W. D. Reiter, U. Hüdepohl, and W. Zillig.** 1992. Elements of an archaeal promoter defined by mutational analysis. Nucleic Acids Res. **20:**5423–5428.
26. **Hering, O., M. Brenneis, J. Beer, B. Suess, and J. Soppa.** 2009. A novel mechanism for translation initiation operates in haloarchaea. Mol. Microbiol. **71:**1451–1463.
27. **Huber, H., M. Gallenberger, U. Jahn, E. Eylert, I. A. Berg, D. Kockelkorn, W. Eisenreich, and G. Fuchs.** 2008. A dicarboxylate/4-hydroxybutyrate autotrophic carbon assimilation cycle in the hyperthermophilic Archaeum *Ignicoccus hospitalis*. Proc. Natl. Acad. Sci. U. S. A. **105:**7851–7856.
28. **Hügler, M., H. Huber, K. O. Stetter, and G. Fuchs.** 2003. Autotrophic CO_2 fixation pathways in archaea (*Crenarchaea*). Arch. Microbiol. **179:**160–173.
29. **Hügler, M., R. S. Krieger, M. Jahn, and G. Fuchs.** 2003. Characterization of acetyl-CoA/propionyl-CoA carboxylase in *Metallosphaera sedula*. Carboxylating enzyme in the 3-hydroxypropionate cycle for autotrophic carbon fixation. Eur. J. Biochem. **270:**736–744.
30. **Jahn, U., H. Huber, W. Eisenreich, M. Hügler, and G. Fuchs.** 2007. Insights into the autotrophic CO_2 fixation pathway of the archaeon *Ignicoccus hospitalis*: comprehensive analysis of the central carbon metabolism. J. Bacteriol. **189:**4108–4119.
31. **Jahn, D., E. Verkamp, and D. Söll.** 1992. Glutamyl-transfer RNA: a precursor of heme and chlorophyll biosynthesis. Trends Biochem. Sci. **17:**215–218.
32. **Kato, N., H. Yurimoto, and R. K. Thauer.** 2006. The physiological role of the ribulose monophosphate pathway in bacteria and archaea. Biosci. Biotechnol. Biochem. **70:**10–21.
33. **King, N. P., T. M. Lee, M. R. Sawaya, D. Cascio, and T. O. Yeates.** 2008. Structures and functional implications of an AMP-binding cystathionine beta-synthase domain protein from a hyperthermophilic archaeon. J. Mol. Biol. **380:**181–192.
34. **Laemmli, U. K.** 1970. Cleavage of structural proteins during the assembly of the head of bacteriophage T4. Nature **227:**680–685.
35. **Littlefield, O., Y. Korkhin, and P. B. Sigler.** 1999. The structural basis for the oriented assembly of a TBP/TFB/promoter complex. Proc. Natl. Acad. Sci. U. S. A. **96:**13668–13673.
36. **Lorentzen, E., R. Hensel, T. Knura, H. Ahmed, and E. Pohl.** 2004. Structural basis of allosteric regulation and substrate specificity of the non-phosphorylating glyceraldehyde 3-phosphate dehydrogenase from *Thermoproteus tenax*. J. Mol. Biol. **341:**815–828.
37. **Marsch, V. L., S. Y. Peak-Chew, and S. D. Bell.** 2008. Sir2 and the acetyltransferase, Pat, regulate the archaeal chromatin protein, Alba. J. Biol. Chem. **380:**21122–21128.
38. **Martins, B. M., H. Dobbek, I. Cinkaya, W. Buckel, and A. Messerschmidt.** 2004. Crystal structure of 4-hydroxybutyryl-CoA dehydratase: radical catalysis involving a [4Fe-4S] cluster and flavin. Proc. Natl. Acad. Sci. U. S. A. **101:**15645–15649.
39. **Moll, I., G. Hirokawa, M. C. Kiel, A. Kaji, and U. Bläsi.** 2004. Translation initiation with 70S ribosomes: an alternative pathway for leaderless mRNAs. Nucleic Acids Res. **32:**3354–3363.
40. **Mowatt, M. R., A. Aggarwal, and T. E. Nash.** 1991. Carboxy-terminal sequence conservation among variant-specific surface proteins of *Giardia lamblia*. Mol. Biochem. Parasitol. **49:**215–227.
41. **Neidhardt, F. C., J. L. Ingraham, and M. Schaechter.** 1990. Physiology of the bacterial cell: a molecular approach. Sinauer Associates, Sunderland, MA.
42. **Orita, I., T. Sato, N. Kato, H. Atomi, T. Imanaka, and Y. Sakai.** 2006. The ribulose monophosphate pathway substitutes for the missing pentose phosphate pathway in the archaeon *Thermococcus kodakaraensis*. J. Bacteriol. **188:**4698–4704.
43. **Palmer, J. R., and C. J. Daniels.** 1995. In vivo definition of an archaeal promoter. J. Bacteriol. **177:**1844–1849.
44. **Paper, W., U. Jahn, M. J. Hohn, M. Kronner, D. J. Näther, T. Burghardt, R. Rachel, K. O. Stetter, and H. Huber.** 2007. *Ignicoccus hospitalis* sp. nov., the host of '*Nanoarchaeum equitans*'. Int. J. Syst. Evol. Microbiol. **57:**803–808.
45. **Qureshi, S. A., and S. P. Jackson.** 1998. Sequence-specific DNA binding by

the *S. shibatae* TFIIB homolog, TFB, and its effect on promoter strength. Mol. Cell **1:**389–400.
46. **Ramos-Vera, W. H., I. A. Berg, and G. Fuchs.** 2009. Autotrophic carbon dioxide assimilation in *Thermoproteales* revisited. J. Bacteriol. **191:**4286–4297.
47. **Reiter, W. D., U. Hüdepohl, and W. Zilling.** 1990. Mutational analysis of an archaebacterial promoter: essential role of a TATA box for transcription efficiency and start-site selection *in vitro*. Proc. Natl. Acad. Sci. U. S. A. **87:**9509–9513.
48. **Rowlands, T., P. Baumann, and S. P. Jackson.** 1994. The TATA-binding protein: a general transcription factor in eukaryotes and archaebacteria. Science **264:**1326–1329.
49. **Schäfer, S., C. Barkowski, and G. Fuchs.** 1986. Carbon assimilation by the autotrophic thermophilic archaebacterium *Thermoproteus neutrophilus*. Arch. Microbiol. **146:**301–308.
50. **Schäfer, S., M. Götz, W. Eisenreich, A. Bacher, and G. Fuchs.** 1989. ^{13}C-NMR study of autotrophic CO_2 fixation in *Thermoproteus neutrophilus*. Eur. J. Biochem. **184:**151–156.
51. **Schäfer, S., T. Paalme, R. Vilu, and G. Fuchs.** 1989. ^{13}C-NMR study of acetate assimilation in *Thermoproteus neutrophilus*. Eur. J. Biochem. **186:**695–700.
52. **Schön, A., G. Krupp, S. Gough, S. Berry-Lowe, C. G. Kannangara, and D. Söll.** 1986. The RNA required in the first step of chlorophyll biosynthesis is a chloroplast glutamate tRNA. Nature **322:**281–284.
53. **Scott, J. W., S. A. Hawley, K. A. Green, M. Anis, G. Stewart, G. A. Scullion, D. G. Norman, and D. G. Hardie.** 2004. CBS domains form energy-sensing modules whose binding of adenosine ligands is disrupted by disease mutations. J. Clin. Invest. **113:**274–284.
54. **Shemin, D., and C. Russel.** 1953. δ-Aminolevulinic acid, its role in the biosynthesis of porphyrins and purines. J. Am. Chem. Soc. **75:**4873–4875.
55. **Slupska, M. M., A. G. King, S. Fitz-Gibbon, J. Besemer, M. Borodovsky, and J. H. Miller.** 2001. Leaderless transcripts of the crenarchaeal hyperthermophile *Pyrobaculum aerophilum*. J. Mol. Biol. **309:**347–360.
56. **Soppa, J.** 1999. Transcription initiation in *Archaea*: facts, factors and future aspects. Mol. Microbiol. **31:**1295–1305.
57. **Strauss, G., W. Eisenreich, A. Bacher, and G. Fuchs.** 1992. ^{13}C-NMR study of autotrophic CO_2 fixation pathways in the sulphur-reducing archaebacterium *Thermoproteus neutrophilus* and in the phototrophic eubacterium *Chloroflexus aurantiacus*. Eur. J. Biochem. **205:**853–866.
58. **Tabor, S., and C. C. Richardson.** 1985. A bacteriophage-T7 RNA-polymerase promoter system for controlled exclusive expression of specific genes. Proc. Natl. Acad. Sci. U. S. A. **82:**1074–1078.
59. **Thomm, M.** 1996. Archaeal transcription factors and their role in transcription initiation. FEMS Microbiol. Rev. **18:**159–171.
60. **Thomm, M., and W. Hausner.** 2007. Transcriptional mechanisms, p. 187–198. *In* R. A. Garrett and H. P. Klenk (ed.), *Archaea*: evolution, physiology, and molecular biology. Blackwell Publishing, Malden, MA.
61. **Tjaden, B., A. Plagens, C. Dörr, B. Siebers, and R. Hensel.** 2006. Phosphoenolpyruvate synthetase and pyruvate, phosphate dikinase of *Thermoproteus tenax*: key pieces in the puzzle of archaeal carbohydrate metabolism. Mol. Microbiol. **60:**287–298.
62. **Tolstrup, N., C. W. Sensen, R. A. Garrett, and I. G. Clausen.** 2000. Two different and highly organized mechanisms of translation initiation in the archaeon *Sulfolobus solfataricus*. Extremophiles **4:**175–179.
63. **Wardleworth, B. N., R. J. Russell, S. D. Bell, G. L. Taylor, and M. F. White.** 2002. Structure of Alba: an archaeal chromatin protein modulated by acetylation. EMBO J. **21:**4654–4662.
64. **Wilson, W. A., S. A. Hawley, and D. G. Hardie.** 1996. Glucose repression/derepression in budding yeast: SNF1 protein kinase is activated by phosphorylation under derepressing conditions, and this correlates with a high AMP: ATP ratio. Curr. Biol. **6:**1426–1434.
65. **Wiśniewski, J. R., A. Zougman, and M. Mann.** 2008. N^{ε}-formylation of lysine is a widespread post-translational modification of nuclear proteins occurring at residues involved in regulation of chromatin function. Nucleic Acids Res. **36:**570–577.
66. **Xue, H., R. Guo, Y. Wenn, D. Liu, and L. Huang.** 2000. An abundant DNA binding protein from the hyperthermophilic archaeon *Sulfolobus shibatae* affects DNA supercoiling in a temperature-dependent fashion. J. Bacteriol. **182:**3929–3933.
67. **Zaparty, M., B. Tjaden, R. Hensel, and B. Siebers.** 2008. The central carbohydrate metabolism of the hyperthermophilic crenarchaeote *Thermoproteus tenax*: pathways and insights into their regulation. Arch. Microbiol. **190:**231–245.
68. **Zaparty, M., A. Zaigler, C. Stamme, J. Soppa, R. Hensel, and B. Siebers.** 2008. DNA microarray analysis of central carbohydrate metabolism: glycolytic/gluconeogenic carbon switch in the hyperthermophilic crenarchaeum *Thermoproteus tenax*. J. Bacteriol. **190:**2231–2238.
69. **Zeikus, J. G., G. Fuchs, W. Kenealy, and R. K. Thauer.** 1977. Oxidoreductases involved in cell carbon synthesis of *Methanobacterium thermoautotrophicum*. J. Bacteriol. **132:**604–613.
70. **Zhao, K., X. Chai, and R. Marmorstein.** 2003. Structure of a Sir2 substrate, Alba, reveals a mechanism for deacetylation-induced enhancement of DNA-binding. J. Biol. Chem. **278:**26071–26077.